Published in final edited form as:
Free Radic Biol Med. 2010 June 1; 48(11): 1501–1512. doi:10.1016/j.freeradbiomed.2010.02.028.

Enhanced expression of mitochondrial superoxide dismutase leads to prolonged *in vivo* cell cycle progression and up-regulation of mitochondrial thioredoxin

Aekyong Kim[a,,1,2], **Suman Joseph**[b,,2], **Aslam Khan**[a], **Charles J Epstein**[b], **Raymond Sobel**[c,,d], and **Ting-Ting Huang**[a,,e,*]

[a]Department of Neurology and Neurological Sciences, Stanford University, Stanford, CA, USA

[b]Department of Pediatrics, University of California, San Francisco, CA, USA

[c]Department of Pathology, Stanford University, Stanford, CA, USA

[d]Laboratory Service, VA Palo Alto Health Care System, Palo Alto, CA, USA

[e]GRECC, VA Palo Alto Health Care System, Palo Alto, CA, USA

Abstract

Mn superoxide dismutase (MnSOD) is an important mitochondrial antioxidant enzyme, and elevated MnSOD levels have been shown to reduce tumor growth in part by suppressing cell proliferation. Studies with fibroblasts have shown that increased MnSOD expression prolongs cell cycle transition time in G1/S and favors entrance into the quiescent state. To determine if the same effect occurs during tissue regeneration *in vivo*, we used a transgenic mouse system with liver-specific MnSOD expression and a partial hepatectomy paradigm to induce synchronized *in vivo* cell proliferation during liver regeneration. We show in this experimental system that a 2.6 fold increase in MnSOD activities leads to delayed entry into S phase, as measured by reduction in bromodeoxyuridine (BrdU) incorporation, and decreased expression of proliferative cell nuclear antigen (PCNA). Thus, compared to control mice with baseline MnSOD levels, transgenic mice with increased MnSOD expression in the liver have 23% fewer BrdU positive cells and a marked attenuation of PCNA expression. The increase in MnSOD activity also leads to an increase of the mitochondrial form of thioredoxin (thioredoxin 2), but not of several other peroxidases examined, suggesting the importance of thioredoxin 2 in maintaining redox balance in mitochondria with elevated levels of MnSOD.

Keywords

MnSOD; partial hepatectomy; mitochondria; thioredoxin 2; liver regeneration; cell cycle progression

[*]Corresponding author: Ting-Ting Huang, Department of Neurology and Neurological Sciences, Stanford University School of Medicine, and GRECC, VA Palo Alto Health Care System, 3801 Miranda Ave. Building 100, D3-101, Palo Alto, CA 94304, USA, Phone 650-496-2581, Fax 650-849-0457 tthuang@stanford.edu.
[1]Current address: School of Pharmacy, Catholic University of Daegu, Gyeongbuk, 712-702, South Korea
[2]These authors contributed equally to this work.

Introduction

Mn superoxide dismutase (MnSOD), one of the three mammalian superoxide dismutases, is encoded by a nuclear gene (*Sod2*) and is then transported into the mitochondrial matrix. It is important for metabolizing superoxide radicals generated from incomplete reduction of oxygen during electron transport, and mutant mice completely deficient in MnSOD cannot survive past the early neonatal period [1]. Increased levels of MnSOD have been shown to be protective against acute oxidative insults such as heart ischemia reperfusion injury [2], MPTP toxicity [3], adriamycin-induced cardiomyopathy [4], and ionizing radiation damage [5–7]. Higher levels of MnSOD have also been shown to confer a longer life span in Drosophila [8,9] and a longer chronological life span in yeast [10]. However the life span extension benefit has not been recapitulated in mammalian model systems [11].

The observation that MnSOD activity is often lower in tumors and transformed cells was made independently by two groups over 30 years ago [12,13]. This prompted Oberley and Buettner to propose that normal cells would become more susceptible to transformation if they lost MnSOD and that addition of SOD to cancer cells would enable them to regain some characteristics of normal cells [14]. Extensive studies have supported these hypotheses and consequently, *Sod2* is often considered to be a tumor suppressor gene [15]. The findings have also been extended to *in vivo* studies with a two-stage skin tumor experimental system [16, 17] and a mouse model of T cell lymphoma [18]. Supplementation of MnSOD or SOD mimetics has also been shown to delay the age of onset as well as the severity of skin tumors [19]. Life-long reduction in MnSOD, on the other hand, leads to increased cancer incidence in mutant mice with reduced MnSOD [20]. Consequently, MnSOD supplementation or enhanced MnSOD expression has been proposed and tested successfully as part of an experimental anti-cancer therapy [21–24].

Tumor suppression by MnSOD has, in part, been attributed to its anti-proliferative effect resulting from changes in the intracellular balance of superoxide and hydrogen peroxide [25, 26]. MnSOD activity correlated directly with cell doubling time and inversely with the plating efficiency and clonogenicity of the tumor cells, which resulted in decreased tumorigenicity in nude mice [15,27]. The inverse correlation between cellular proliferative potential and MnSOD activity also applies to nonmalignant cells [26,28,29]. MnSOD activities change in different stages of cell proliferation and differentiation, with less MnSOD in S phase than that in G0 phase [30] and lower MnSOD in undifferentiated cells than in differentiated cells [31]. Studies also showed that up-regulation of MnSOD leads to a prolonged G1/S phase in the cell cycle [26], and that increased MnSOD favors cell quiescence [32].

Much of the work on antiproliferative effects of MnSOD has been carried out *in vitro*, and it is not clear if the same applies *in vivo* during normal tissue regeneration. Since MnSOD supplementation may be a promising ancillary anti-cancer treatment, it is important to know how it may affect normal tissue regeneration. In this study, we use a tetracycline-inducible system to achieve liver-specific expression of MnSOD in transgenic mice and a partial hepatectomy paradigm for synchronized *in vivo* cell proliferation to examine the role of enhanced MnSOD expression in cell cycle progression and antioxidant balance during liver regeneration.

Methods

Generation of double transgenic mice for liver-specific expression of *Sod2*-TRE-*LacZ*

To create an inducible MnSOD expression construct, an 11 kb promoterless mouse MnSOD (*Sod2*) genomic fragment containing the transcription initiation codon and the entire coding sequence was isolated from a previously derived genomic clone [33] and inserted downstream

of a bi-directional tet-responsive promoter (Figure 1). The bi-directional promoter controls LacZ expression in the opposite direction, and induction of LacZ can be used as an indicator for the expression of MnSOD from the same promoter. A DNA fragment containing the entire *Sod2*-TRE-*LacZ* sequence was isolated from the cloning vector (pBI-G, GeneBank Accession number, U89933) and microinjected into fertilized B6D2F1 eggs for transgenic mouse production. Microinjection was carried out by the transgenic core facility at the University of California, San Francisco.

Sod2-TRE-*LacZ* transgenic mice were backcrossed to C57BL/6J mice for 2–3 generations before they were used for this study. Transgenic mice expressing a liver-specific transactivator (LAP-tTA) were originally obtained from the Jackson Laboratory [34,35]. LAP-tTA is capable of activating the transgenes on its own and the activation can be suppressed in the presence of doxycycline (DOX). LAP-tTA transgenic line was crossed with *Sod2*-TRE-*LacZ* to generate double transgenic (*Sod2*-TRE-*LacZ* transgenic with LAP-tTA transgene), single transgenic (*Sod2*-TRE-*LacZ* transgenic or LAP-tTA transgenic), and non-transgenic mice within the same breeding. To suppress *Sod2*-TRE-*LacZ* expression, double transgenic mice were fed Dox supplemented (1,000 ppm in Purina 5001) mouse chow for 14 days. At the time the breeding was carried out to generate mice for this study, *Sod2*-TRE-*LacZ* was on a mixed C57BL/6J;DBA/2 background and LAP-tTA was on a mixed FVB/N;C57BL/6J background. All animal handling procedures were approved by the IACUC committees at the University of California, San Francisco and at the VA Palo Alto Health Care System.

Enzyme activity measurements

Gel-based activity measurements—MnSOD and CuZnSOD in liver lysates were separated by non-denaturing isoelectric focusing gel electrophoresis (Ampholine PAGplate, pH 3.5–9.5, Amersham Pharmacia Biotech, Inc. Piscataway, NJ), and activities were determined with a nitroblue tetrazolium staining solution as described previously [36]. Sixty to 150 μg total protein per lane from liver tissue lysates were used for the analysis. The activity stain creates clear bands on a dark purple background and identifies the location of MnSOD and CuZnSOD in the gel. Cytosolic and mitochondrial aconitase (ACO1 and ACO2) and NADP-dependent isocitreate dehydrogenase (IDH1 and IDH2) were separated by cellulose acetate gel (Cellogel, 250–300 μ, Accurate Chemical and Scientific Corporation, Westbury, NY) electrophoresis at 200 volts for 15 minutes, and activities were determined with a MTT/PMS staining solution as described [36,37]. The activity stain creates dark purple bands on a white background and identifies the location of the mitochondrial and the cytosolic form of each enzyme. The band intensity, which is proportional to the enzyme activity, was quantified by Image J 1.36b (NIH, USA) and normalized to total protein loading. To control for gel to gel variations in the activity stain, liver from an unoperated single Tg female mouse was loaded in every gel. All data are expressed as a percentage of the standard sample described above.

Colorimetric assays—Glutathione reductase (GR) activities were determined by the decrease in NADPH concentration [38] using the Glutathione Reductase Assay Kit from Assay Designs/Stressgen (Ann Arbor, MI). A standard curve, generated with purified GR ranging from 0.5 to 20 mU, was used to calculate specific GR activities in each sample. Total glutathione S-transferase (GST) activity in liver lysates was determined by measuring the conjugation of 1-chloro-2,4-dinitrobenzene (CDNB) with reduced glutathione [39] using the Glutathione S-Transferase Assay Kit from Cayman Chemical (Ann Arbor, MI). The CDNB extinction coefficient, adjusted for the path length of the solution in the well, of 0.00503 $\mu M^{-1}cm^{-1}$ was used. Enzyme activities were normalized to total protein, triplicate assays were carried out for each sample.

Partial Hepatectomy

Sod2-TRE-*LacZ*/LAP-tTA double transgenic mice (double Tg) have constitutively increased expression of MnSOD in liver when they are fed with normal mouse chow and are used as the liver-specific MnSOD transgenic mice. Single transgenic *Sod2*-TRE-*LacZ* (single Tg) mice generated as littermates of doubleTg were used as control mice with basal level expression of MnSOD. Partial hepatectomy was performed following the procedures of Greene and Puder [40]. The average age was 11.6 ± 1.8 weeks (mean ± SD) at the time of surgery, and the surgeries were always performed between 9 and 11 am. Mice were sedated by an i.p. injection of Ketamine (120 mg/kg) and Xylazine (8 mg/kg), and anesthetized during surgery under a constant flow of 2% isofluorane delivered through a nose cone. Sixty-70% of liver was surgically removed from each mouse. To prevent infection, 5 gm/kg of Baytril was injected once after surgery. To minimize pain, 0.1 mg/kg Buprenorphine was injected (i.p.) every 12 hours until the mice were euthanized for tissue collection. It has been well documented that the number of BrdU positive cells peaks about 40 hours after partial hepatectomy in mice [41,42]. Therefore, to catch the first round of cell replication, we injected bromodeoxyuridine (BrdU, 50 mg/kg) in PBS (10 mg/ml, pH 7.2) into the intraperitoneal cavity at 39 hours and euthanized the mice 2 hours later for tissue collection. Liver samples collected during surgeries were designated as the 0-hour samples and those collected at 2 hours after BrdU injection were designated as the 41-hour samples.

Tissue processing for hematoxylin and eosin (H&E) staining and BrdU immunostaining

A small sample (approximately 1 cm^3 in size) of liver was fixed in 10% neutral buffered formalin at room temperature for 24 hours and stored in 70% ethanol at 4°C prior to processing for paraffin embedding. Four μm sections were prepared on histology slides. Before H&E and BrdU staining, sections were heated in a 55°C oven for 10 seconds, deparaffinized in xylene for 10 minutes, rehydrated through a series of descending concentrations of alcohol, and rinsed three times in PBS (pH 7.2). For histologic analysis, the sections were stained with H&E and evaluated by light microscopy based on the extent of necrotic areas and the size and amount of lipid droplets (Supplemental Figure 2).

For BrdU immunohistochemical staining, sections were incubated with 10% methanol, 3% hydrogen peroxide solution in PBS (pH7.2) for 30 minutes followed by washing three times in PBS. The sections were then processed at room temperature (RT) sequentially with a 200 μg/ml pepsin solution in PBS containing 0.01 N HCl for 30 minutes, 2 N HCl for 45 minutes, 100 mM borax solution (pH 8.5) for 10 minutes, and PBS for 10 minutes, and then blocked with 3% normal rat serum in PBS containing 0.1% Triton-X (PBST) for 30 minutes. Incubation with primary antibody was carried out at 4°C overnight in a humid chamber using a rat monoclonal antibody against BrdU (Table 1). Sections were washed three times in PBS for 5 minutes each at RT, and treated with biotinylated secondary antibody (Table 1) in PBST containing 1% normal rat serum for 3 hours at RT. After three washes in PBS for 5 minutes each, stain was visualized using the Vectastain Elite ABC Kit (PK-6100, Vector Laboratories) according to manufacturer's recommendations. Nuclei were counter-stained with hematoxylin (H-3404, Vector Laboratories). Sections were mounted with cover slips and the BrdU immunostaining of nuclei was evaluated by light microscopy using a 20x objective. Six random, non-overlapping areas were counted for BrdU positive and negative cells from each sample, and the percentage of BrdU positive cells over total cell population was calculated. Small intestines, which continuously renew epithelial cells at the base of the crypts, were collected from each BrdU injected mouse to serve as a positive control for BrdU immunohistochemical staining. Samples with no BrdU positive staining in the small intestines were excluded. The investigators conducting the histological evaluations and BrdU cell counts were blinded to the genotypes of the samples.

Western blot analyses

To determine changes in antioxidant enzymes, proteins involved in redox balance, proteins involved in a few signaling pathways, and the extent of protein nitration in livers after partial hepatectomy, western blot analyses were carried out. A piece of flesh-frozen liver from each sample was homogenized in Mammalian Protein Extraction Reagent (M-PER, Pierce, USA) containing a protease inhibitor cocktail (P2714, Sigma, USA) and phosphatase inhibitor cocktail 1 (P2750, Sigma) at 20 μl per mg tissue. After centrifugation at 10,000 g for 5 minutes at 4°C, supernatants were aliquoted and stored at −80°C. Total protein concentration was measured using the Bradford method (Bio-Rad, USA). Thirty μg of total protein was separated by the NuPAGE gel system (Invitrogen, USA) and transferred to a PVDF membrane for western blot analyses. Membranes were blocked in 5% nonfat-milk/PBST solution (PBS containing 0.05 % Tween 20, pH 7.2) and incubated sequentially with primary antibody and horseradish peroxidase-conjugated secondary antibody (Table 1). Signals were detected using ECL Plus Reagent and Typhoon 9410 and quantified using ImageQuant software version 5.0 (Amersham Bioscience Corp., USA). Primary and secondary antibodies used in this study are listed in Table 1. The signal intensity of each band was normalized to that of β-actin. Liver from an unoperated single Tg female mouse was used as a standard sample and was included in each membrane to control for the inherent variance among membranes during western blot processing and analysis. All data are expressed as a percentage of the standard sample described above.

Statistical analyses

The statistical analysis program GraphPad Prism (version 4.03, GraphPad Software, Inc., San Diego, CA, USA) was used for data analyses. Student's t test was used to determine differences between males and females and between single and double Tg. Within each experimental group, comparisons between males and females were first carried out to determine gender-based difference in the parameter examined. If there was no gender-based difference, data from male and female mice were combined and compared between single and double Tg. Otherwise, comparisons were carried out within each gender. The paired t test was used to determine differences between 0 and 41 hours within each genotype. Two-way ANOVA was carried out to determine possible interactions between genotype and gender (genotype x gender) and between genotype and time (genotype x time).

Results

Characterization of *Sod2*-TRE-*LacZ* expression in double transgenic mice

Sod2-TRE-*LacZ*/LAP-tTA double Tg mice showed a liver-specific expression with an 18-fold difference in β-galactosidase activities between double Tg mice treated with and without Dox (Supplemental Figure 1). No significant changes in β-galactosidase activities were detected in other tissues from double Tg mice treated with or without Dox. Enzymatic activities measured from samples collected at various stages of this study showed a 2.6-fold increase in MnSOD activities in the liver of *Sod2*-TRE-*LacZ*/LAP-tTA double Tg mice (Figure 3), and the activities paralleled increase in MnSOD protein level (Figure 3 and Figure 5). The discrepancy in the magnitude of increase between β-galactosidase and MnSOD activities in *Sod2*-TRE-*LacZ*/LAP-tTA double Tg liver is likely due to the difference in the baseline level of each enzyme in single Tg controls, in which β-galactosidase from the transgene is not expected to be expressed and endogenous β-galactosidase is not active at the pH the activity assay is carried out.

Histopathological evaluation of livers after partial hepatectomy

We performed partial hepatectomy on a total of 61 mice. The gender and genotype segregation followed the expected Mendelian inheritance pattern (Supplemental Table 1). Body weights were measured before and at 41 hours post surgery; weights of the livers that were removed during the surgery and recovered at 41 hours post surgery were also recorded. Based on the histopathological assessments on the 41-hour liver samples, partially hepatectomized mice can be divided into two groups: mice with good histopathological outcomes with no obvious necrosis or with mild necrosis in less than 25% of areas examined, and mice with bad histopathological outcomes with severe necrosis in more than 50% of areas examined with compromised cellular structure (Supplemental Table 1). There were no significant differences between the two groups in most of the parameters measured, except for the extent of body weight loss measured at 41 hours post surgery. Mice with a good histopathological outcome at 41 hours post surgery lost an average of 8.03±0.64% of their pre-surgery body weight, whereas mice with a bad histopathological outcome lost 11.45±0.59% of their pre-surgery body weight ($p=0.0002$). Samples with severe necrosis accompanied by completely disintegrated cellular structure often showed no BrdU positive nuclear staining (data not shown). About 44% of mice fell into the bad outcome category, but gender and genotype were not related to the outcome and the cause of necrosis was not clear. All BrdU and all downstream studies were restricted to samples either without necrosis or with mild necrosis in less than 25% of the inspected area.

Reduced percentage of BrdU positive hepatocytes and PCNA expression in *Sod2*-TRE-*LacZ*/LAP-tTA double Tg mice

BrdU incorporation into hepatocytes was evaluated as a proliferative index at 41 hours after partial hepatectomy. A total of 1889 ± 350 cells were counted from each sample with 315 ± 58 cells per area. The percentage of BrdU positive cells in double Tg mice was 23% lower than that in *Sod2*-TRE-*LacZ* single Tg controls (29.4 ± 2.5% vs. 37.9 ± 2.6% BrdU positive cells, $p=0.0237$, Figure 2B). Consistent with the BrdU results, PCNA expression in double Tg mice only went up by 2.8 fold at 41 hours after partial hepatectomy, whereas PCNA expression in single Tg mice went up by 6.4 fold (Figure 2D). These results indicate that hepatocytes with increased MnSOD expression have attenuated proliferative capabilities during liver regeneration after partial hepatectomy. No gender-based differences in the number of BrdU positive cells or PCNA expression was observed within each genotype.

Antioxidant enzyme profiles

We screened 1) nine antioxidant enzymes [CuZnSOD (SOD1), MnSOD (SOD2), EC-SOD (SOD3), peroxiredoxin 1 (PRDX1), peroxiredoxin 3 (PRDX3), thioredoxin 1 (TXN1), thioredoxin 2 (TXN2), glutathione peroxidase (GPX1), and catalase (CAT)]; 2) two proteins related to NADPH generation in the mitochondria [nicotinamide nucleotide transhydrogenase (NNT) and NADP-dependent isocitrate dehydrogenase (IDH2)]; and 3) cytosolic and mitochondrial aconitase (ACO1 and ACO2) by western blot analyses. With the exception of NNT, which was present at a very low level in the liver and could not be reliably quantified, all proteins levels were normalized first to β-actin within each individual sample then to the unoperated single Tg control common to all membranes (see **Methods**) and compared between genders, genotypes, and treatment groups. In addition to western blot analyses, activity assays were carried out to determine specific activities of SOD1, SOD2, ACO1, ACO2, IDH1, IDH2, total glutathione S-transferase (GST), and glutathione reductase (GR).

Tight regulation of antioxidant enzymes in double Tg mice—Of the antioxidant enzymes examined by western blot and/or activity analyses, only MnSOD and TXN2 are increased in double Tg mice. There were no gender differences in the protein levels of these

two enzymes. On average, MnSOD protein levels in double Tg were 63% and 53% higher than in single Tg mice at 0 and 41 hours, respectively (Figure 3A). TXN2 protein levels in double Tg mice on the other hand, were 40% and 82% higher than that in single Tg mice at 0 and 41 hours, respectively (Figure 3B). Protein levels for both enzymes were decreased at 41 hours after partial hepatectomy. However, the extent of reduction in MnSOD was larger in double Tg, whereas the reduction in TXN2 was larger in single Tg mice. In contrast, activity measurements of MnSOD showed no decrease in activities after partial hepatectomy (Figure 3C).

Aconitase activities are reduced in double Tg at baseline—Cytosolic (ACO1) and mitochondrial (ACO2) aconitase activities were measured to determine changes in compartment-specific oxidative stress in single and double Tg mice after partial hepatectomy. Double Tg mice showed a 30% reduction in ACO1 and ACO2 activities at 0 hour (Figure 4) when compared to single Tg mice. However, the relationship was reversed after partial hepatectomy and ACO2 activity was 40% lower in single Tg mice. No significant difference in ACO1 activities between single and double Tg mice was detected at 41 hours.

Partial hepatectomy leads to reduced protein levels—With a few exceptions, partial hepatectomy led to across the board reduction in protein levels, and the reduction was not limited to a specific subcellular compartment (see below). The extent of reduction ranged from 9.7% to 34.7%. Four enzymes show significant reduction in both single and double Tg. They are SOD1, SOD2, PRDX1, and IDH2 (Figure 5) with SOD1 and PRDX1 belonging to the cytosolic compartment and SOD2 and IDH2 belonging to the mitochondrial compartment. In addition, TXN2 and GPX1 showed a significant reduction in single Tg, whereas SOD3 showed a significant reduction in double Tg only (data not shown). Furthermore, paired t test between samples collected at 0 and 41 hours from the same mouse showed a more frequent and severe reduction in male mice. Proteins that did not show a significant difference between 0 and 41 hours include ACO1, ACO2, CAT, PRDX3, and TXN1 (data not shown). In contrast to changes in protein levels, enzyme activity measurements on SOD1, SOD2, and IDH2 showed no remarkable differences between 0 and 41 hours (Figure 3C).

Gender differences in antioxidant protein profiles—Several proteins measured by western blot analyses showed significant gender effects by two-way ANOVA, and they include SOD3, PRDX1, PRDX3, TXN1, IDH2, and ACO2. In general, female mice have higher protein levels than males in the same genotype and treatment group. Enzyme activity measurements on IDH2 showed a similar gender effect with female mice having higher enzyme activities than males (data not shown). Analyses of genotype x gender interactions showed significant interactions at both 0 and 41 hours in PRDX1 and TXN1 (Figure 6), and only at 0 hour in PRDX3 and at 41 hours in SOD3. No significant genotype x time interaction was identified in any of the proteins examined. GR and total GST activities also showed a significant gender effect (Figure 7). However, in contrast to the proteins mentioned above, male mice have higher GR and total GST activities than females in the same genotype and treatment group.

Nitrotyrosine formation

To determine the extent of oxidative protein modification, we measured the level of nitrotyrosine formation in the liver samples by western blot analysis. There were two major bands identified by nitrotyrosine antibody at about 58 kD and 26 kD range. For the final data analysis, we quantified and normalized the signal intensity of these two bands for comparison across all samples. There were no significant gender- or genotype-based differences. However, there were significant reductions in the 58 kD band in the 41-hour samples in both genotypes (Figure 8). A similar trend was also observed in the 26 kD band, although statistical significance was only present in single Tg males and double Tg females. The time effect accounts for 37.8%

and 26.6% of variation observed in the 58 kD and 26 kD band, respectively. The identity of the 58 and 26 kD nitrotyrosine positive proteins are unknown.

Changes in signaling pathways

To identify signaling pathways associated with MnSOD-mediated attenuation of hepatocyte proliferation after partial hepatectomy, two pairs of representative samples (single and double Tg) were screened using a commercial antibody microarray (Kinex™ antibody microarray service, Kinexus, Vancouver, Canada), which focused on the regulation of proteins involved in signal transduction. The results suggested attenuations in 1) proliferation, 2) apoptosis, and the 3) MAP kinase, 4) PI3K, and 5) IRS/IGFR signaling pathways and enhancement of the Wnt/β-Catenin signaling pathway in MnSOD overexpressing mice (data not shown). A few representative proteins in each signaling pathway were then tested with the entire set of samples by western blotting. These proteins (Table 1) included insulin receptor substrate 1 (IRS-1), β-Arrestin 1, casein kinase 1ε, extracellular regulated kinases (ERK1/2), phosphoinositide 3-kinase (PI3K) p110α, retinoblastoma protein (Rb), and p34 cell division cycle 2 (Cdc2). No statistically significant differences between single and double Tg were observed in any of the proteins examined (data not shown).

Discussion

In this study, we created and characterized a tetracycline-inducible MnSOD transgenic mouse line and used partial hepatectomy as an experimental system to determine the effects of MnSOD on cell cycle progression in an *in vivo* environment. We showed that up-regulation of MnSOD in the liver by 2.6 fold led to a significant decrease in cell proliferation and in the number of cells entering S phase after partial hepatectomy. We also showed that up-regulation of MnSOD led to a concomitant increase in thioredoxin 2 (TXN2). Although partial hepatectomy led to active cell proliferation, it also led to decreased expression of multiple cellular proteins and the change was not limited to the mitochondrial compartment. Finally, based on antioxidant enzyme profiles, male and female mice may rely on different antioxidant systems for ROS removal.

A number of transgenic mice overexpressing MnSOD have been generated in the last two decades [18,33,43–47]. These include tissue-specific and ubiquitous expression of MnSOD with expression levels ranging from roughly 60% to 20 fold above non-transgenic control levels. In all cases, control of transgene expression is limited to the promoters used to drive the transgenes, and there is very little flexibility in controlling the timing of transgene expression. A binary transgenic system such as the tetracycline-inducible system used in this study, on the other hand, allows the flexibility in controlling the timing of transgene expression and in directing transgene expression in different tissues by combining with tissue-specific transactivator transgenic mice. The on/off switch of MnSOD expression is particularly important, given the diverse effects of MnSOD on cell proliferation and differentiation and on cell survival and tumor cell metastasis.

In this experimental system, the level of MnSOD was only increased by 2.6 fold in double Tg mice, and yet, the number of cells entering S phase (BrdU positive cells) was 23% lower than that in control mice (Figure 2B). A concomitant reduction in PCNA expression suggests that lower BrdU index in double Tg mice was not because MnSOD overexpressing hepatocytes progressed through cell cycle faster and had already passed the S phase when BrdU was injected. A previous study showed that an 8-fold increase in MnSOD activity in androgen-independent human prostate cancer cells resulted in a decrease in the number of cells in S-phase as measured by BrdU incorporation (39.9% in control vs. 28.5% in MnSOD overexpressing cells) [22]. An 80% increase in MnSOD activity in NIH/3T3 cells also led to an 11% decrease in the number of cells in S-phase (34.6% in control vs. 23.7% in MnSOD

overexpressing cells) [28]. Results from these reports are comparable with that from this study (37.9% in control vs. 29.4% in MnSOD overexpressing hepatocytes) and suggests a consistent effect of elevated levels of MnSOD on cell cycle progression in both the *in vitro* and *in vivo* environments.

It has been suggested that redox imbalance due to MnSOD-mediated elevation of H_2O_2 may account for growth inhibition in malignant cells [25] or the delay in cell cycle progression in nonmalignant cells [26]. As an affirmation to that notion, increased expression of catalase in mitochondria or cytosol was able to reverse the MnSOD-mediated inhibition of proliferation and reduce the steady-state H_2O_2 levels in HT-1080 fibrosarcoma cells [48]. In addition, when overexpression of MnSOD was forced on either non-malignant or malignant cells *in vitro*, clones with increased MnSOD expression often had altered expression, as an adaptive response, in other antioxidant enzymes, such as decreased CuZnSOD and increased glutathione peroxidase or catalase activities [22,25,28,29,49]. Independently from these biological experiments, Buettner et al show the contribution of MnSOD to the flux of H_2O_2 in cells by measuring the rate of H_2O_2 release into culture medium from cells with differing levels of MnSOD followed by kinetic modeling [50]. These results imply that there may be a maximum level of MnSOD activity that cells can tolerate without compromising normal cellular physiology and mitochondrial integrity, and that increased H_2O_2-removing capacity may help in withstanding elevated MnSOD activity by reducing H_2O_2 toxicity.

Up-regulation of peroxidases in MnSOD overexpressing transgenic mice, on the other hand, has not been reported perhaps because only a limited number of peroxidases, mainly catalase and glutathione peroxidase, have been investigated either by western blotting or by direct enzyme activity assay so far. In this study, we again showed that there was no significant change in catalase and glutathione peroxidase 1 protein levels in MnSOD overexpressing mice. However, with our investigation of an expanded panel of peroxidase families, we have shown that mice with higher levels of MnSOD also had a parallel increase in the mitochondrial form of thioredoxin (thioredoxin 2, TNX2), whereas levels of cytosolic thioredoxin (thioredoxin 1, or TXN1) and mitochondrial peroxiredoxin (peroxiredoxin 3, or PRDX3) were not significantly altered. Similar to this finding, an earlier *in vitro* study demonstrated a tight temporal correlation between MnSOD induction and *Txn2* transcriptional up-regulation [51]. This was likely a result of the need to re-establish the redox balance in the mitochondrial compartment due to increased H_2O_2 production from excess amounts of MnSOD, as introduction of an antioxidant into mitochondria dampened transcriptional induction of *Txn2* [50]. The TXN2 result also underscores the importance of thioredoxin system in maintaining an optimal mitochondrial redox environment.

TXN2, a 12 kD disulfide reductase, is part of the thiol-reducing system in mitochondria and its role is to reduce PRDX3, which removes mitochondrially-generated H_2O_2 [52]. Oxidized TXN2 is then reduced by thioredoxin reductase 2 [52]. The presence of TXN2 is critical for cell survival, since homozygous TXN2 knockout (*Txn2*-/-) mice die during mid-gestation between embryonic day 10.5 and 12.5 [53]; fetal fibroblasts derived from *Txn2*-/- embryos are not viable in culture [53]; and TXN2-deficient cells undergo spontaneous apoptosis [54]. Heterozygous *Txn2* knockout mice also show impaired mitochondrial function, increased production of ROS, and enhanced sensitivity to oxidative stress [55]. On the other hand, higher levels of TXN2 confer protection, in most cases, against conditions of oxidative stress [56–61] even though some contradicting results from *in vitro* studies exist [59,62]. TXN2 is constitutively expressed at high levels in tissues with high metabolic rates [63], and expression of TXN2 has been shown to increase in muscles from senescent and caloric restricted mice and in cells treated with H_2O_2 [64,65]. However, the mechanism underlying up-regulation of *Txn2* is mostly unknown. Up-regulation of TXN2, but not TXN1, in the present experiment suggests that there is a compartment-specific requirement for enhancing H_2O_2 metabolism

within mitochondria. Up-regulation of TXN2, but not of PRDX3, within the thiol-reducing pathway also implies that there may be a preference in ramping up production of this small thiol protein in response to increased MnSOD. Whether the preference for TXN2 over PRDX3 is due to the efficiency in producing smaller proteins (TXN2, 12 kD vs. PRDX3, 28 kD), or a more responsive *Txn2* promoter to H_2O_2 signaling in not clear.

Aconitases are iron-sulfur containing enzymes and are very sensitive to direct inactivation by O_2^-, H_2O_2, and $ONOO^-$ [66–69]. Even though there was no significant difference in ACO1 and ACO2 protein levels between single and double Tg mice at 0 and 41 hours, reduced ACO1 and ACO2 activities was observed in double Tg mice (Figure 4) at 0 hour. The data suggests that, even with a compensatory increase in TXN2, a 2.6 fold increase in MnSOD activity leads to increased oxidative stress in the cytosol and mitochondria. The data is consistent with the notion that increased MnSOD expression leads to increased H_2O_2 production [32,48,50], which then leads to increased inactivation of aconitases. Single Tg mice showed a ~40% reduction in ACO1 and ACO2 activities at 41 hours after partial hepatictomy, suggesting an increase in oxidative stress in both cytosolic and mitochondrial compartments during this early stage of tissue regeneration. Double Tg mice, on the other hand, did not have a further reduction in ACO1 activities after partial hepatectomy, and ACO2 activities in double Tg mice actually improved by 45%. The data implied a lower level of ROS in the mitochondria in double Tg mice during the initial period of tissue regeneration. Whether the improved ACO2 activities reflect a more reduced environment in the mitochondria will need to be confirmed with independent assays on other redox-sensitive proteins.

It is interesting that the two-way ANOVA showed a significant gender effect in the protein levels of four antioxidant enzymes (SOD3, PRDX1, PRDX3, and TXN1) and two mitochondrial proteins (IDH2 and ACO2), as well as in the specific activities of four enzymes (IDH2, ACO2, GR, and GST) examined in this study. Female mice tend to have higher protein levels in the peroxiredoxin/thioredoxin pathway (PRDX1, PRDX3, and TXN1, Figure 6), whereas male mice have higher enzyme activities in the glutathione/glutathione reductase pathway (GR and GST, Figure 7). Even though our examination of these two pathways was not exhaustive, the results underscored a possible difference in redox regulations between male and female mice. Despite these differences, there were no gender differences in the number of BrdU positive cells or PCNA expression levels (Figure 2), nor was there difference in partial hepatectomy outcome (Table 1). The data suggest that peroxiredoxin/thioredoxin and glutathione/glutathione reductase pathways are probably equally important in redox regulation and consequently, rendering the same outcome in cell cycle progression under conditions of MnSOD overexpression. Among this group of proteins, only PRDX1 and TXN1 showed interaction between gender and genotype. PRDX1 levels were significantly higher in single transgenic females (i.e. non-MnSOD overexpressors) than single Tg males, and the difference was diminished in double Tg mice (Figure 6, upper panel). On the other hand, TXN1 levels were higher only in double transgenic females, but not in single transgenics (Figure 6, lower panel). This contradictory genotype x gender interaction between two enzymes of the same thiol reducing pathway suggests that, within the context of this experimental system, controls of PRDX1 and TXN1 expression in female mice may be independent of each other. Alternatively, increase in MnSOD level may have a dichotomy effect on PRDX1 and TXN1 in female mice only.

A large number of proteins analyzed in this study showed a significant reduction at 41 hours after partial hepatectomy, and this was not limited to proteins in a specific subcellular compartment, nor was it related to a specific genotype. With the exception of protein nitration products (the 58 and 26 kD bands), we were examining proteins that belonged to antioxidant or metabolic systems. It is possible that during tissue regeneration cellular resources need to be diverted for the production of “building blocks” for rapid tissue expansion. Consequently,

expression of non-structural proteins may be selectively down regulated to increase production of essential structural proteins, and differences in MnSOD and other proteins would have no bearing on this shift. The reduction in nitrotyrosine levels after partial hepatectomy (Figure 8) was more likely a reflection of the selective down regulation of non-structural proteins, rather than an indication of reduced oxidative stress. The lack of concordance between changes in protein levels and enzyme activities in SOD1, SOD2, and IDH2 after partial hepatectomy could be due to the ROS-sensitive nature of these enzymes [70–73] and as a result, not all proteins have full enzyme activities. It is also possible that the discrepancy is due to the nature of the activity measurement approach. These enzymes were separated by non-denaturning IEF gel or cellulose acetate gel followed by activity staining. The methods have a narrower linear range for signal detection and a higher level of gel-to-gel variations when compared to western blot analyses. Consequently, the sensitivity for detecting changes in specific activities may be lower than the conventional kinetic assays carried out with a spectrophotomer.

A step-wise effort was carried out to identify candidate signaling pathways responsible for the delay in cell cycle progression and suppression of cell replication in MnSOD overexpressing mice during liver regeneration. Even though our initial screen with two pairs of samples identified some candidate signaling pathways, subsequent screening of all the samples with a few selected members in each pathway by western blotting failed to lead to any firm conclusion. This was probably because only a few proteins and their phosphorylation status in each pathway were tested. A more extensive study will be necessary to identify signaling pathway(s) involved in MnSOD-mediated delay in cell cycle progression and/or suppression of cell replication.

MnSOD is an important mitochondrial antioxidant enzyme. Its catalytic activity leads to changes in the balance of O_2^- and H_2O_2 and in turns, alters cellular physiology. On the one hand, presence of MnSOD is protective against O_2^- toxicity, and up-regulation of MnSOD mediated by FOXO3a protects quiescent cells from oxidative stress [74]. The presence of MnSOD is necessary to protect the proliferative capacity of confluent normal human fibroblasts [75], and increased MnSOD expression reduces chromosomal instability, thereby reducing tumor onset in a T cell lymphoma mouse model [18]. Therefore, a major challenge in generalizing about MnSOD as a tumor suppressor protein may arise from the fact that MnSOD acts as a pro-survival protein and can protect cancer cells against chemotherapeutic agents that rely on generation of reactive oxygen species for their cytotoxicity [76]. On the other hand, up-regulation of MnSOD without accompanying H_2O_2-removing capacity results in onset of spontaneous apoptosis [77,78], and increased mitochondrial H_2O_2 generation from elevated levels of MnSOD activity is responsible for reduced cell proliferation and entrance into the quiescence phase of cell cycle in mouse fibroblasts [26,32,79]. Consequently, a combination of enhanced MnSOD activity and reduced H_2O_2 removing capacity has been shown to be quite effective in inhibiting tumor growth in nude mice [24]. In the clinical setting though it would be difficult, if not impossible, to administer anticancer agents only within the tumor proper without affecting the surrounding normal tissues. Therefore, MnSOD-based tumor therapy needs to take into consideration its potential impact on normal tissue survival, repair, and regeneration. More complete knowledge of the response to elevated MnSOD levels in normal tissues vs. malignant tissues will be beneficial in applying MnSOD-based tumor therapies to suppress and eradicate tumor growth and at the same time, maintain or enhance the repair and regeneration of surrounding normal tissues.

Supplementary Material

Refer to Web version on PubMed Central for supplementary material.

Acknowledgments

We thank Xinli Wang for excellent animal care and Laura Gigliello at the Veterinary Medicine Unit for the instruction on partial hepatectomy procedure. This work was supported by funding from the National Institutes of Health (AG24400 and AG16998), Stanford Cancer Council, and Stanford Digestive Disease Center, and by the resources and facilities at the VA Palo Alto Health Care System.

List of Abbreviations

ACO1	cytosolic aconitase
ACO2	mitochondrial aconitase
BrdU	bromodeoxyuridine
CAT	catalase
CuZnSOD	CuZn superoxide dismutase (SOD1)
EC-SOD	extracellular superoxide dismutase (SOD3)
GPX1	glutathione peroxidase 1
GPX4	glutathione peroxidase 4 (PhGPX4)
GR	glutathione reductase
GST	glutathione S-transferase
IDH1	cytosolic NADP-dependent isocitrate dehydrogenase
IDH2	mitochondrial NADP-dependent isocitrate dehydrogenase
LAP	liver-enriched activator protein
MnSOD	Mn superoxide dismutase (SOD2)
NNT	nicotinamide nucleotide transhydrogenase
PCNA	proliferative cell nuclear antigen
PRDX1	peroxiredoxin 1
PRDX3	peroxiredoxin 3
PRDX-SO3	peroxiredoxin, sulfonic form
Sod2	gene encoding Mn superoxide dismutase
Tet-Of	suppresses transgene expression in the presence of tetracycline and its analogues
Tg mouse	transgenic mouse
TRE	tetracycline response element
tTA	transactivator for tetracycline response element
TXN1	thioredoxin 1
TXN2	thioredoxin 2
Txn2	gene encoding thioredoxin 2

References

1. Li Y, Huang TT, Carlson EJ, Melov S, Ursell PC, Olson JL, Noble LJ, Yoshimura MP, Berger C, Chan PH, Wallace DC, Epstein CJ. Dilated cardiomyopathy and neonatal lethality in mutant mice lacking manganese superoxide dismutase. Nat Genet 1995;11:376–381. [PubMed: 7493016]

2. Chen Z, Siu B, Ho YS, Vincent R, Chua CC, Hamdy RC, Chua BH. Overexpression of MnSOD protects against myocardial ischemia/reperfusion injury in transgenic mice. J Mol Cell Cardiol 1998;30:2281–2289. [PubMed: 9925365]
3. Klivenyi P, St Clair D, Wermer M, Yen HC, Oberley T, Yang L, Flint Beal M. Manganese superoxide dismutase overexpression attenuates MPTP toxicity. Neurobiol Dis 1998;5:253–258. [PubMed: 9848095]
4. Yen HC, Oberley TD, Gairola CG, Szweda LI, St Clair DK. Manganese superoxide dismutase protects mitochondrial complex I against adriamycin-induced cardiomyopathy in transgenic mice. Arch Biochem Biophys 1999;362:59–66. [PubMed: 9917329]
5. Epperly MW, Kagan VE, Sikora CA, Gretton JE, Defilippi SJ, Bar-Sagi D, Greenberger JS. Manganese superoxide dismutase-plasmid/liposome (MnSOD-PL) administration protects mice from esophagitis associated with fractionated radiation. Int J Cancer 2001;96:221–231. [PubMed: 11474496]
6. Carpenter M, Epperly MW, Agarwal A, Nie S, Hricisak L, Niu Y, Greenberger JS. Inhalation delivery of manganese superoxide dismutase-plasmid/liposomes protects the murine lung from irradiation damage. Gene Ther 2005;12:685–693. [PubMed: 15750616]
7. Zhang X, Epperly MW, Kay MA, Chen ZY, Dixon T, Franicola D, Greenberger BA, Komanduri P, Greenberger JS. Radioprotection in vitro and in vivo by minicircle plasmid carrying the human manganese superoxide dismutase transgene. Hum Gene Ther 2008;19:820–826. [PubMed: 18699723]
8. Sun J, Folk D, Bradley TJ, Tower J. Induced overexpression of mitochondrial Mn-superoxide dismutase extends the life span of adult Drosophila melanogaster. Genetics 2002;161:661–672. [PubMed: 12072463]
9. Sun J, Molitor J, Tower J. Effects of simultaneous over-expression of Cu/ZnSOD and MnSOD on Drosophila melanogaster life span. Mech Ageing Dev 2004;125:341–349. [PubMed: 15130751]
10. Harris N, Costa V, MacLean M, Mollapour M, Moradas-Ferreira P, Piper PW. Mnsod overexpression extends the yeast chronological (G(0)) life span but acts independently of Sir2p histone deacetylase to shorten the replicative life span of dividing cells. Free Radic Biol Med 2003;34:1599–1606. [PubMed: 12788479]
11. Perez VI, Van Remmen H, Bokov A, Epstein CJ, Vijg J, Richardson A. The overexpression of major antioxidant enzymes does not extend the lifespan of mice. Aging Cell 2009;8:73–75. [PubMed: 19077044]
12. Dionisi O, Galeotti T, Terranova T, Azzi A. Superoxide radicals and hydrogen peroxide formation in mitochondria from normal and neoplastic tissues. Biochim Biophys Acta 1975;403:292–300. [PubMed: 241399]
13. Sahu SK, Oberley LW, Stevens RH, Riley EF. Superoxide dismutase activity of Ehrlich ascites tumor cells. J Natl Cancer Inst 1977;58:1125–1128. [PubMed: 845983]
14. Oberley LW, Buettner GR. Role of superoxide dismutase in cancer: a review. Cancer Res 1979;39:1141–1149. [PubMed: 217531]
15. Oberley LW. Mechanism of the tumor suppressive effect of MnSOD overexpression. Biomed Pharmacother 2005;59:143–148. [PubMed: 15862707]
16. Zhao Y, Xue Y, Oberley TD, Kiningham KK, Lin SM, Yen HC, Majima H, Hines J, St Clair D. Overexpression of manganese superoxide dismutase suppresses tumor formation by modulation of activator protein-1 signaling in a multistage skin carcinogenesis model. Cancer Res 2001;61:6082–6088. [PubMed: 11507057]
17. Zhao Y, Oberley TD, Chaiswing L, Lin SM, Epstein CJ, Huang TT, St Clair D. Manganese superoxide dismutase deficiency enhances cell turnover via tumor promoter-induced alterations in AP-1 and p53-mediated pathways in a skin cancer model. Oncogene 2002;21:3836–3846. [PubMed: 12032821]
18. van de Wetering CI, Coleman MC, Spitz DR, Smith BJ, Knudson CM. Manganese superoxide dismutase gene dosage affects chromosomal instability and tumor onset in a mouse model of T cell lymphoma. Free Radic Biol Med 2008;44:1677–1686. [PubMed: 18291119]
19. Zhao Y, Chaiswing L, Oberley TD, Batinic-Haberle I, St Clair W, Epstein CJ, St Clair D. A mechanism-based antioxidant approach for the reduction of skin carcinogenesis. Cancer Res 2005;65:1401–1405. [PubMed: 15735027]

20. Van Remmen H, Ikeno Y, Hamilton M, Pahlavani M, Wolf N, Thorpe SR, Alderson NL, Baynes JW, Epstein CJ, Huang TT, Nelson J, Strong R, Richardson A. Life-long reduction in MnSOD activity results in increased DNA damage and higher incidence of cancer but does not accelerate aging. Physiol Genomics 2003;16:29–37. [PubMed: 14679299]
21. Weydert C, Roling B, Liu J, Hinkhouse MM, Ritchie JM, Oberley LW, Cullen JJ. Suppression of the malignant phenotype in human pancreatic cancer cells by the overexpression of manganese superoxide dismutase. Mol Cancer Ther 2003;2:361–369. [PubMed: 12700280]
22. Venkataraman S, Jiang X, Weydert C, Zhang Y, Zhang HJ, Goswami PC, Ritchie JM, Oberley LW, Buettner GR. Manganese superoxide dismutase overexpression inhibits the growth of androgen-independent prostate cancer cells. Oncogene 2005;24:77–89. [PubMed: 15543233]
23. Weydert CJ, Waugh TA, Ritchie JM, Iyer KS, Smith JL, Li L, Spitz DR, Oberley LW. Overexpression of manganese or copper-zinc superoxide dismutase inhibits breast cancer growth. Free Radic Biol Med 2006;41:226–237. [PubMed: 16814103]
24. Weydert CJ, Zhang Y, Sun W, Waugh TA, Teoh ML, Andringa KK, Aykin-Burns N, Spitz DR, Smith BJ, Oberley LW. Increased oxidative stress created by adenoviral MnSOD or CuZnSOD plus BCNU (1,3-bis(2-chloroethyl)-1-nitrosourea) inhibits breast cancer cell growth. Free Radic Biol Med 2008;44:856–867. [PubMed: 18155673]
25. Ridnour LA, Oberley TD, Oberley LW. Tumor suppressive effects of MnSOD overexpression may involve imbalance in peroxide generation versus peroxide removal. Antioxid Redox Signal 2004;6:501–512. [PubMed: 15130277]
26. Kim A, Zhong W, Oberley TD. Reversible modulation of cell cycle kinetics in NIH/3T3 mouse fibroblasts by inducible overexpression of mitochondrial manganese superoxide dismutase. Antioxid Redox Signal 2004;6:489–500. [PubMed: 15130276]
27. Zhang HJ, Yan T, Oberley TD, Oberley LW. Comparison of effects of two polymorphic variants of manganese superoxide dismutase on human breast MCF-7 cancer cell phenotype. Cancer Res 1999;59:6276–6283. [PubMed: 10626823]
28. Li N, Oberley TD, Oberley LW, Zhong W. Inhibition of cell growth in NIH/3T3 fibroblasts by overexpression of manganese superoxide dismutase: mechanistic studies. J Cell Physiol 1998;175:359–369. [PubMed: 9572481]
29. Li N, Oberley TD. Modulation of antioxidant enzymes, reactive oxygen species, and glutathione levels in manganese superoxide dismutase-overexpressing NIH/3T3 fibroblasts during the cell cycle. J Cell Physiol 1998;177:148–160. [PubMed: 9731755]
30. Oberley TD, Schultz JL, Li N, Oberley LW. Antioxidant enzyme levels as a function of growth state in cell culture. Free Radic Biol Med 1995;19:53–65. [PubMed: 7635359]
31. Erlejman AG, Oteiza PI. The oxidant defense system in human neuroblastoma IMR-32 cells predifferentiation and postdifferentiation to neuronal phenotypes. Neurochem Res 2002;27:1499–1506. [PubMed: 12512954]
32. Sarsour EH, Venkataraman S, Kalen AL, Oberley LW, Goswami PC. Manganese superoxide dismutase activity regulates transitions between quiescent and proliferative growth. Aging Cell 2008;7:405–417. [PubMed: 18331617]
33. Raineri I, Carlson EJ, Gacayan R, Carra S, Oberley TD, Huang TT, Epstein CJ. Strain-dependent high-level expression of a transgene for manganese superoxide dismutase is associated with growth retardation and decreased fertility. Free Radic Biol Med 2001;31:1018–1030. [PubMed: 11595386]
34. Mansuy IM, Winder DG, Moallem TM, Osman M, Mayford M, Hawkins RD, Kandel ER. Inducible and reversible gene expression with the rtTA system for the study of memory. Neuron 1998;21:257–265. [PubMed: 9728905]
35. Kistner A, Gossen M, Zimmermann F, Jerecic J, Ullmer C, Lubbert H, Bujard H. Doxycycline-mediated quantitative and tissue-specific control of gene expression in transgenic mice. Proc Natl Acad Sci U S A 1996;93:10933–10938. [PubMed: 8855286]
36. Huang TT, Raineri I, Eggerding F, Epstein CJ. Transgenic and mutant mice for oxygen free radical studies. Methods Enzymol 2002;349:191–213. [PubMed: 11912909]
37. Hebert, PD.; Beaton, MJ. Methodologies for allozyme analysis using cellulose acetate electrophoresis -- A practical handbook. Helena Laboratories; 1989.

38. Carlberg I, Mannervik B. Glutathione reductase. Methods Enzymol 1985;113:484–490. [PubMed: 3003504]
39. Pabst MJ, Habig WH, Jakoby WB. Glutathione S-transferase A. A novel kinetic mechanism in which the major reaction pathway depends on substrate concentration. J Biol Chem 1974;249:7140–7147. [PubMed: 4436301]
40. Greene AK, Puder M. Partial hepatectomy in the mouse: technique and perioperative management. J Invest Surg 2003;16:99–102. [PubMed: 12746193]
41. Weglarz TC, Sandgren EP. Timing of hepatocyte entry into DNA synthesis after partial hepatectomy is cell autonomous. Proc Natl Acad Sci U S A 2000;97:12595–12600. [PubMed: 11050176]
42. DeAngelis RA, Markiewski MM, Taub R, Lambris JD. A high-fat diet impairs liver regeneration in C57BL/6 mice through overexpression of the NF-kappaB inhibitor, IkappaBalpha. Hepatology 2005;42:1148–1157. [PubMed: 16231352]
43. Ho YS, Vincent R, Dey MS, Slot JW, Crapo JD. Transgenic models for the study of lung antioxidant defense: enhanced manganese-containing superoxide dismutase activity gives partial protection to B6C3 hybrid mice exposed to hyperoxia. Am J Respir Cell Mol Biol 1998;18:538–547. [PubMed: 9533942]
44. Epperly MW, Travis EL, Whitsett JA, Raineri I, Epstein CJ, Greenberger JS. Overexpression of manganese superoxide dismutase (MnSOD) in whole lung or alveolar type II cells of MnSOD transgenic mice does not provide intrinsic lung irradiation protection. Int J Cancer 2001;96:11–21. [PubMed: 11241326]
45. Chen H, Li X, Epstein PN. MnSOD and catalase transgenes demonstrate that protection of islets from oxidative stress does not alter cytokine toxicity. Diabetes 2005;54:1437–1446. [PubMed: 15855331]
46. Shen X, Zheng S, Metreveli NS, Epstein PN. Protection of cardiac mitochondria by overexpression of MnSOD reduces diabetic cardiomyopathy. Diabetes 2006;55:798–805. [PubMed: 16505246]
47. Goto H, Nishikawa T, Sonoda K, Kondo T, Kukidome D, Fujisawa K, Yamashiro T, Motoshima H, Matsumura T, Tsuruzoe K, Araki E. Endothelial MnSOD overexpression prevents retinal VEGF expression in diabetic mice. Biochem Biophys Res Commun 2008;366:814–820. [PubMed: 18083119]
48. Rodriguez AM, Carrico PM, Mazurkiewicz JE, Melendez JA. Mitochondrial or cytosolic catalase reverses the MnSOD-dependent inhibition of proliferation by enhancing respiratory chain activity, net ATP production, and decreasing the steady state levels of H(2)O(2). Free Radic Biol Med 2000;29:801–813. [PubMed: 11063906]
49. Ough M, Lewis A, Zhang Y, Hinkhouse MM, Ritchie JM, Oberley LW, Cullen JJ. Inhibition of cell growth by overexpression of manganese superoxide dismutase (MnSOD) in human pancreatic carcinoma. Free Radic Res 2004;38:1223–1233. [PubMed: 15621700]
50. Buettner GR, Ng CF, Wang M, Rodgers VG, Schafer FQ. A new paradigm: manganese superoxide dismutase influences the production of H2O2 in cells and thereby their biological state. Free Radic Biol Med 2006;41:1338–1350. [PubMed: 17015180]
51. Kim A, Murphy MP, Oberley TD. Mitochondrial redox state regulates transcription of the nuclear-encoded mitochondrial protein manganese superoxide dismutase: a proposed adaptive response to mitochondrial redox imbalance. Free Radic Biol Med 2005;38:644–654. [PubMed: 15683720]
52. Ahsan MK, Lekli I, Ray D, Yodoi J, Das DK. Redox Regulation of Cell Survival by Thioredoxin Super-family: An Implication of Redox Gene Therapy in the Heart. Antioxid Redox Signal. 2009
53. Nonn L, Williams RR, Erickson RP, Powis G. The absence of mitochondrial thioredoxin 2 causes massive apoptosis, exencephaly, and early embryonic lethality in homozygous mice. Mol Cell Biol 2003;23:916–922. [PubMed: 12529397]
54. Tanaka T, Hosoi F, Yamaguchi-Iwai Y, Nakamura H, Masutani H, Ueda S, Nishiyama A, Takeda S, Wada H, Spyrou G, Yodoi J. Thioredoxin-2 (TRX-2) is an essential gene regulating mitochondria-dependent apoptosis. EMBO J 2002;21:1695–1703. [PubMed: 11927553]
55. Perez VI, Lew CM, Cortez LA, Webb CR, Rodriguez M, Liu Y, Qi W, Li Y, Chaudhuri A, Van Remmen H, Richardson A, Ikeno Y. Thioredoxin 2 haploinsufficiency in mice results in impaired mitochondrial function and increased oxidative stress. Free Radic Biol Med 2008;44:882–892. [PubMed: 18164269]

56. Chen Y, Cai J, Murphy TJ, Jones DP. Overexpressed human mitochondrial thioredoxin confers resistance to oxidant-induced apoptosis in human osteosarcoma cells. J Biol Chem 2002;277:33242–33248. [PubMed: 12032145]
57. Chen Y, Cai J, Jones DP. Mitochondrial thioredoxin in regulation of oxidant-induced cell death. FEBS Lett 2006;580:6596–6602. [PubMed: 17113580]
58. Chen Y, Yu M, Jones DP, Greenamyre JT, Cai J. Protection against oxidant-induced apoptosis by mitochondrial thioredoxin in SH-SY5Y neuroblastoma cells. Toxicol Appl Pharmacol 2006;216:256–262. [PubMed: 16797630]
59. Chen Y, Go YM, Pohl J, Reed M, Cai J, Jones DP. Increased mitochondrial thioredoxin 2 potentiates N-ethylmaleimide-induced cytotoxicity. Chem Res Toxicol 2008;21:1205–1210. [PubMed: 18447393]
60. Dai S, He Y, Zhang H, Yu L, Wan T, Xu Z, Jones D, Chen H, Min W. Endothelial-specific expression of mitochondrial thioredoxin promotes ischemia-mediated arteriogenesis and angiogenesis. Arterioscler Thromb Vasc Biol 2009;29:495–502. [PubMed: 19150880]
61. Widder JD, Fraccarollo D, Galuppo P, Hansen JM, Jones DP, Ertl G, Bauersachs J. Attenuation of angiotensin II-induced vascular dysfunction and hypertension by overexpression of Thioredoxin 2. Hypertension 2009;54:338–344. [PubMed: 19506101]
62. Damdimopoulos AE, Miranda-Vizuete A, Pelto-Huikko M, Gustafsson JA, Spyrou G. Human mitochondrial thioredoxin. Involvement in mitochondrial membrane potential and cell death. J Biol Chem 2002;277:33249–33257. [PubMed: 12080052]
63. Jurado J, Prieto-Alamo MJ, Madrid-Risquez J, Pueyo C. Absolute gene expression patterns of thioredoxin and glutaredoxin redox systems in mouse. J Biol Chem 2003;278:45546–45554. [PubMed: 12954614]
64. Rohrbach S, Gruenler S, Teschner M, Holtz J. The thioredoxin system in aging muscle: key role of mitochondrial thioredoxin reductase in the protective effects of caloric restriction? Am J Physiol Regul Integr Comp Physiol 2006;291:R927–R935. [PubMed: 16675629]
65. De Zoysa M, Pushpamali WA, Whang I, Kim SJ, Lee J. Mitochondrial thioredoxin-2 from disk abalone (Haliotis discus discus): molecular characterization, tissue expression and DNA protection activity of its recombinant protein. Comp Biochem Physiol B Biochem Mol Biol 2008;149:630–639. [PubMed: 18255328]
66. Gardner PR, Fridovich I. Inactivation-reactivation of aconitase in Escherichia coli. A sensitive measure of superoxide radical. J Biol Chem 1992;267:8757–8763. [PubMed: 1315737]
67. Hausladen A, Fridovich I. Superoxide and peroxynitrite inactivate aconitases, but nitric oxide does not. J Biol Chem 1994;269:29405–29408. [PubMed: 7961919]
68. Hausladen A, Fridovich I. Measuring nitric oxide and superoxide: rate constants for aconitase reactivity. Methods Enzymol 1996;269:37–41. [PubMed: 8791635]
69. Rouault TA, Klausner RD. The impact of oxidative stress on eukaryotic iron metabolism. EXS 1996;77:183–197. [PubMed: 8856975]
70. Kwon OJ, Lee SM, Floyd RA, Park JW. Thiol-dependent metal-catalyzed oxidation of copper, zinc superoxide dismutase. Biochim Biophys Acta 1998;1387:249–256. [PubMed: 9748611]
71. Lee SM, Huh TL, Park JW. Inactivation of NADP(+)−dependent isocitrate dehydrogenase by reactive oxygen species. Biochimie 2001;83:1057–1065. [PubMed: 11879734]
72. Macmillan-Crow LA, Cruthirds DL. Invited review: manganese superoxide dismutase in disease. Free Radic Res 2001;34:325–336. [PubMed: 11328670]
73. Alvarez B, Demicheli V, Duran R, Trujillo M, Cervenansky C, Freeman BA, Radi R. Inactivation of human Cu,Zn superoxide dismutase by peroxynitrite and formation of histidinyl radical. Free Radic Biol Med 2004;37:813–822. [PubMed: 15304256]
74. Kops GJ, Dansen TB, Polderman PE, Saarloos I, Wirtz KW, Coffer PJ, Huang TT, Bos JL, Medema RH, Burgering BM. Forkhead transcription factor FOXO3a protects quiescent cells from oxidative stress. Nature 2002;419:316–321. [PubMed: 12239572]
75. Sarsour EH, Agarwal M, Pandita TK, Oberley LW, Goswami PC. Manganese superoxide dismutase protects the proliferative capacity of confluent normal human fibroblasts. J Biol Chem 2005;280:18033–18041. [PubMed: 15743756]

76. Cho SJ, Park JW, Kang JS, Kim WH, Juhnn YS, Lee JS, Kim YH, Ko YS, Nam SY, Lee BL. Nuclear factor-kappaB dependency of doxorubicin sensitivity in gastric cancer cells is determined by manganese superoxide dismutase expression. Cancer Sci 2008;99:1117–1124. [PubMed: 18384434]

77. Bernard D, Quatannens B, Begue A, Vandenbunder B, Abbadie C. Antiproliferative and antiapoptotic effects of crel may occur within the same cells via the up-regulation of manganese superoxide dismutase. Cancer Res 2001;61:2656–2664. [PubMed: 11289144]

78. Kim A, Oberley LW, Oberley TD. Induction of apoptosis by adenovirus-mediated manganese superoxide dismutase overexpression in SV-40-transformed human fibroblasts. Free Radic Biol Med 2005;39:1128–1141. [PubMed: 16214029]

79. Oberley LW, Oberley TD, Buettner GR. Cell division in normal and transformed cells: the possible role of superoxide and hydrogen peroxide. Med Hypotheses 1981;7:21–42. [PubMed: 6259499]

80. Zou Y, Chen CH, Fike JR, Huang TT. A new mouse model for temporal- and tissue-specific control of extracellular superoxide dismutase. Genesis 2009;47:142–154. [PubMed: 19165829]

81. Chen OS, Schalinske KL, Eisenstein RS. Dietary iron intake modulates the activity of iron regulatory proteins and the abundance of ferritin and mitochondrial aconitase in rat liver. J Nutr 1997;127:238–248. [PubMed: 9039823]

82. Schalinske KL, Blemings KP, Steffen DW, Chen OS, Eisenstein RS. Iron regulatory protein 1 is not required for the modulation of ferritin and transferrin receptor expression by iron in a murine pro-B lymphocyte cell line. Proc Natl Acad Sci U S A 1997;94:10681–10686. [PubMed: 9380695]

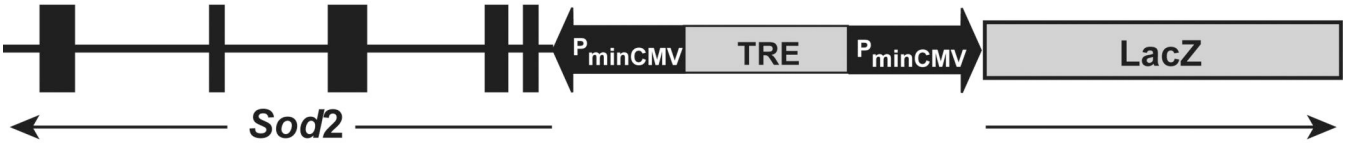

Figure 1.
Inducible MnSOD (*Sod2*) expression construct under the control of a bi-directional tet-responsive element (TRE). The thick vertical bars in *Sod2* represent the five exons and the horizontal line represents the intron sequence. The arrows indicate the orientations of *Sod2* and *LacZ*. The drawing is not to the scale.

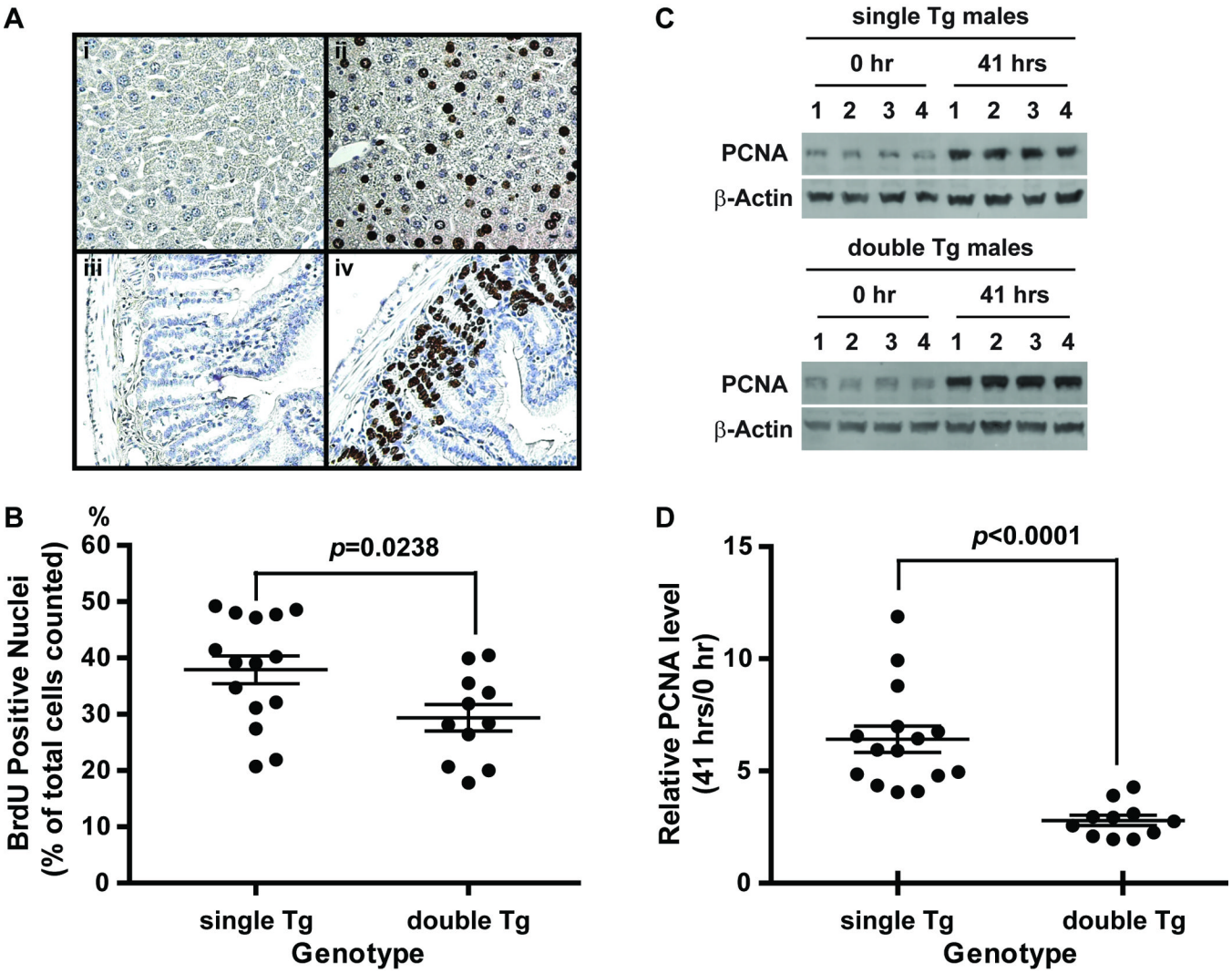

Figure 2.

BrdU and PCNA analysis of liver samples from partial hepatectomy. A, Images of BrdU staining in liver and small intestine recovered at 41 hours post surgery. Representative BrdU positive sections (ii and iv) and negative controls (i and iiI) are shown. BrdU positive cells showed intense brown color in the nuclei interspersed among hepatocytes (ii) and at the base of the crypts of the small intestine lining (iv). Sections were counter stained with hematoxylin. Small intestines were used as positive controls for BrdU injection and immunostaining. Negative controls (i and iii) for BrdU immunostaining were carried out without the primary antibody. B, Percentage of BrdU positive cells in livers recovered at 41 hours post surgery from single and double Tg mice. C, PCNA levels determined by western blot analysis. Representative results from 4 each independent pairs of liver samples collected at 0 hour and 41 hours post surgery from male single and double Tg mice are shown. D, the ratio of PCNA levels between 0 hour and 41 hours. Single Tg, *Sod2*-TRE-*LacZ* single transgenic mice; double Tg, *Sod2*-TRE-*LacZ*/LAP-tTA double Tg mice. Single Tg, n=15 (11 males and 4 females); double Tg, n=11 (4 males and 7 females). Scatter plots show individual values and horizontal lines indicate mean ± SEM in B and D.

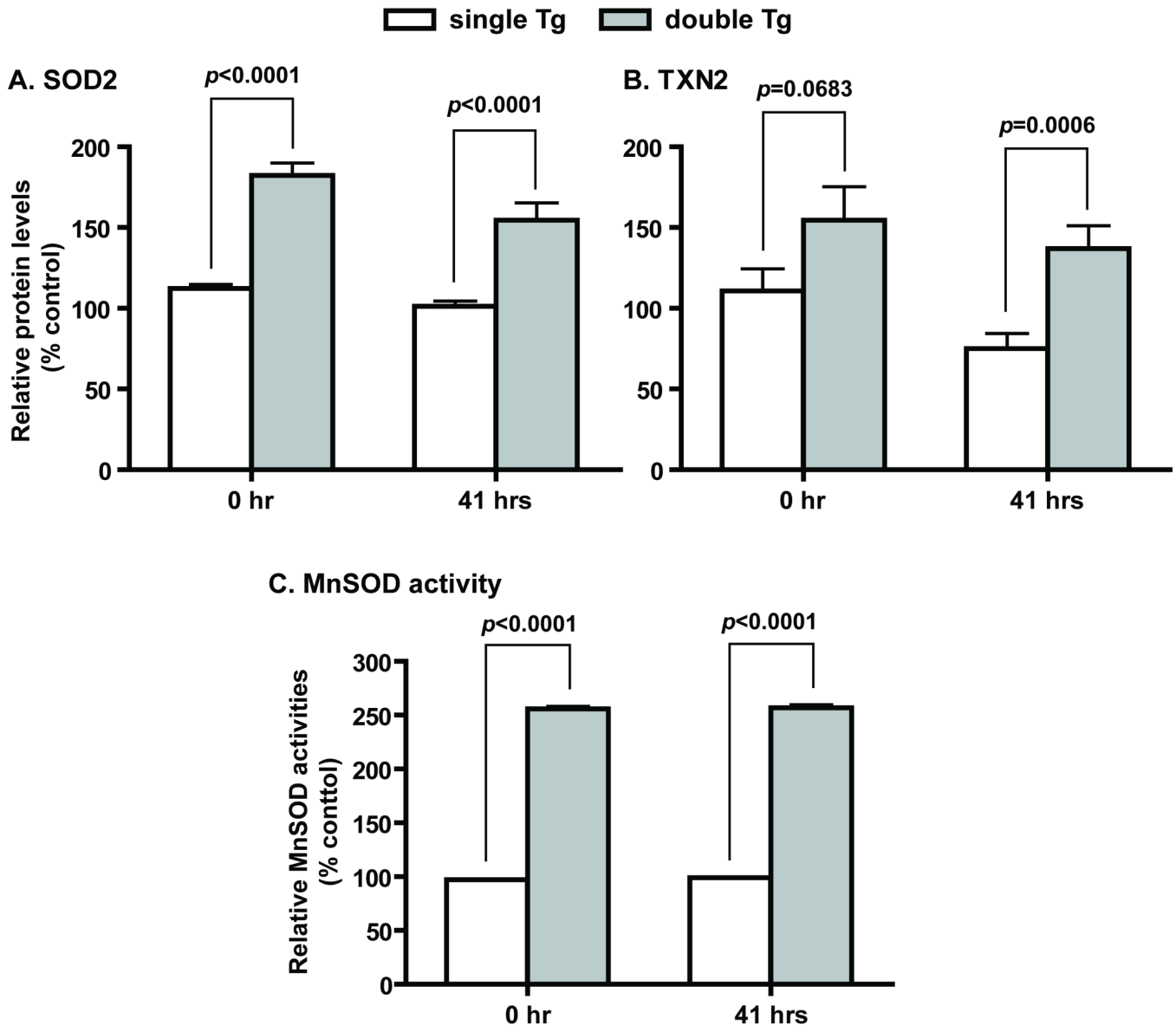

Figure 3.

Increased expression of MnSOD and TXN2 in *Sod2*-TRE-*LacZ*/LAP-tTA double Tg mice. A and B, MnSOD and TXN2 protein levels determined by western blot analyses. Single Tg, n=15 (11 males and 4 females); double Tg, n=11 (4 males and 7 females). C, MnSOD activities determined by non-denaturing IEF gel electrophoresis followed by activity staining. Single Tg, n=8 (4 males and 4 females); double Tg, n=11 (4 males and 7 females). SOD2 and TXN2 are protein designations for MnSOD and thioredoxin 2, respectively. Mean ± SEM of normalized signal intensity are shown. Error bars are too small to show in the activity figure. Student's t test was carried out for the comparison between single and double Tg at each time point.

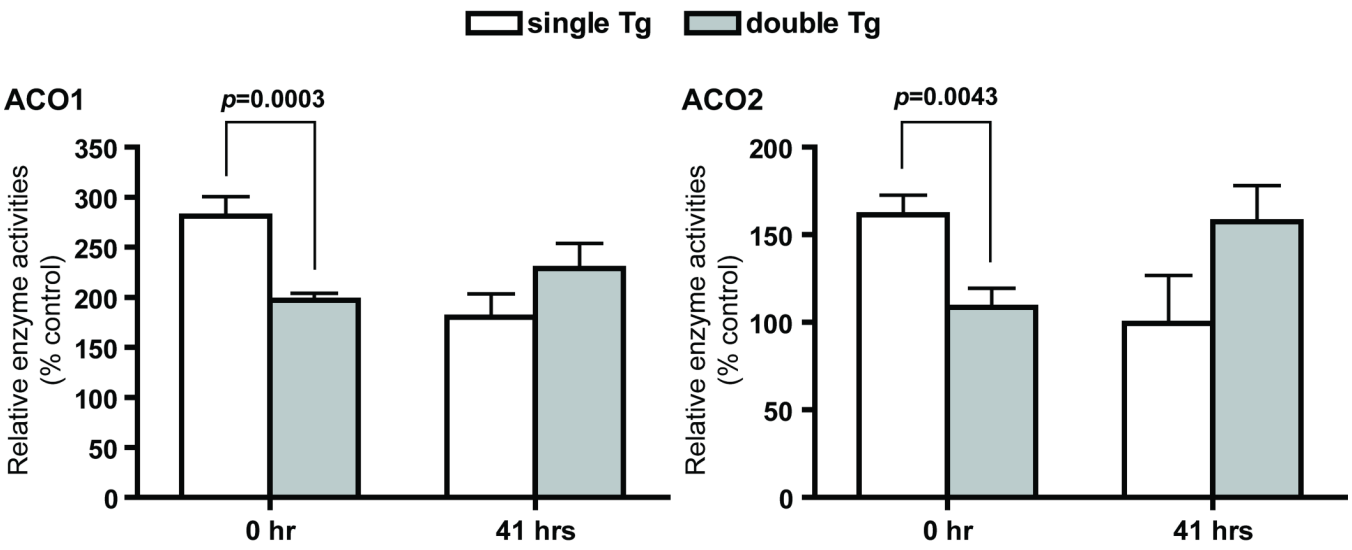

Figure 4.

Changes in cytosolic and mitochondrial aconitase activities. ACO1 and ACO2 were separated by cellulose acetate gel electrophoresis followed by activity staining. Single Tg, n=8 (4 males and 4 females); double Tg, n=11 (4 males and 7 females). ACO1 and ACO2 are protein designations for cytosolic aconitase and mitochondrial aconitase, respectively. Mean ± SEM of normalized signal intensity are shown.

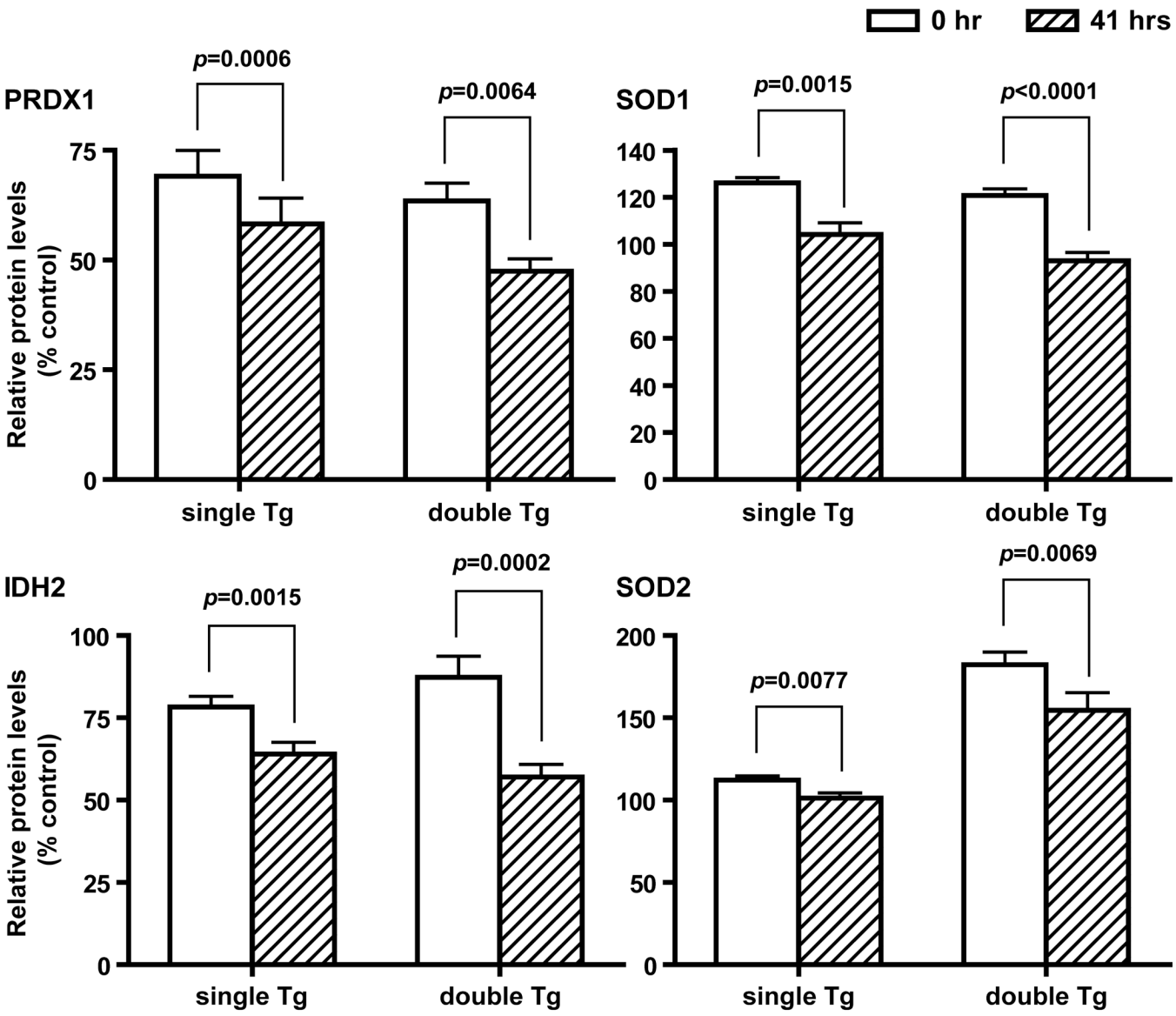

Figure 5.

Decreased antioxidant protein levels after partial hepatectomy. Proteins that show a significant reduction in both single and double Tg mice at 41 hours post surgery are shown. Mean ± SEM of normalized western blot signals are shown. Single Tg, n=15 (11 males and 4 females); double Tg, n=11 (4 males and 7 females). PRDX1, SOD1, IHD2, and SOD2 are protein designations for peroxiredoxin 1, CuZnSOD, isocitrate dehydrogenase 2 (NADP-dependent), and MnSOD, respectively. Paired t test was carried out for the comparison between 0- and 41-hour samples within each genotype.

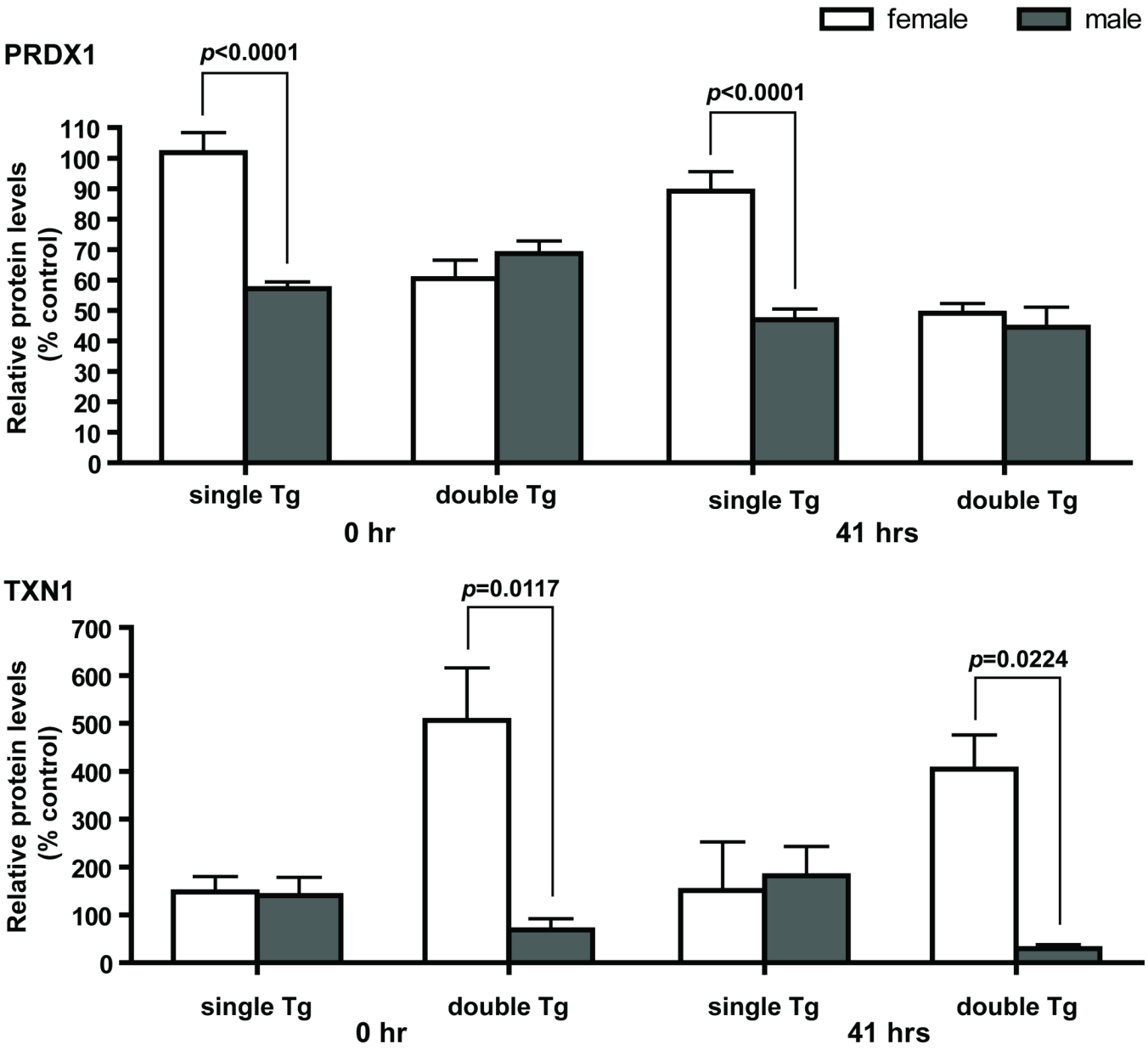

Figure 6.

Gender and genotype interaction affects PRDX1 and TXN1 levels at both time points. Upper panel, significant differences in PRDX1 protein levels between males and females were observed in single Tg mice. At both 0 and 41 hours, male single Tg mice have less than 60% of PRDX1 found in female single Tg mice. No significant differences were observed between male and female double Tg mice. Lower panel, significant differences in TXN1 protein levels between males and females were observed in double Tg mice. TXN1 levels in male double Tg mice are only 15% and 8% of that in female double Tg mice, respectively. No significant difference in TXN1 level between males and females was observed in single Tg mice. Single Tg, n=15 (11 males and 4 females); double Tg, n=11 (4 males and 7 females). Two-way ANOVA was used to determine interaction between gender and genotype; Student's t test was used for the comparison between males and females within each genotype.

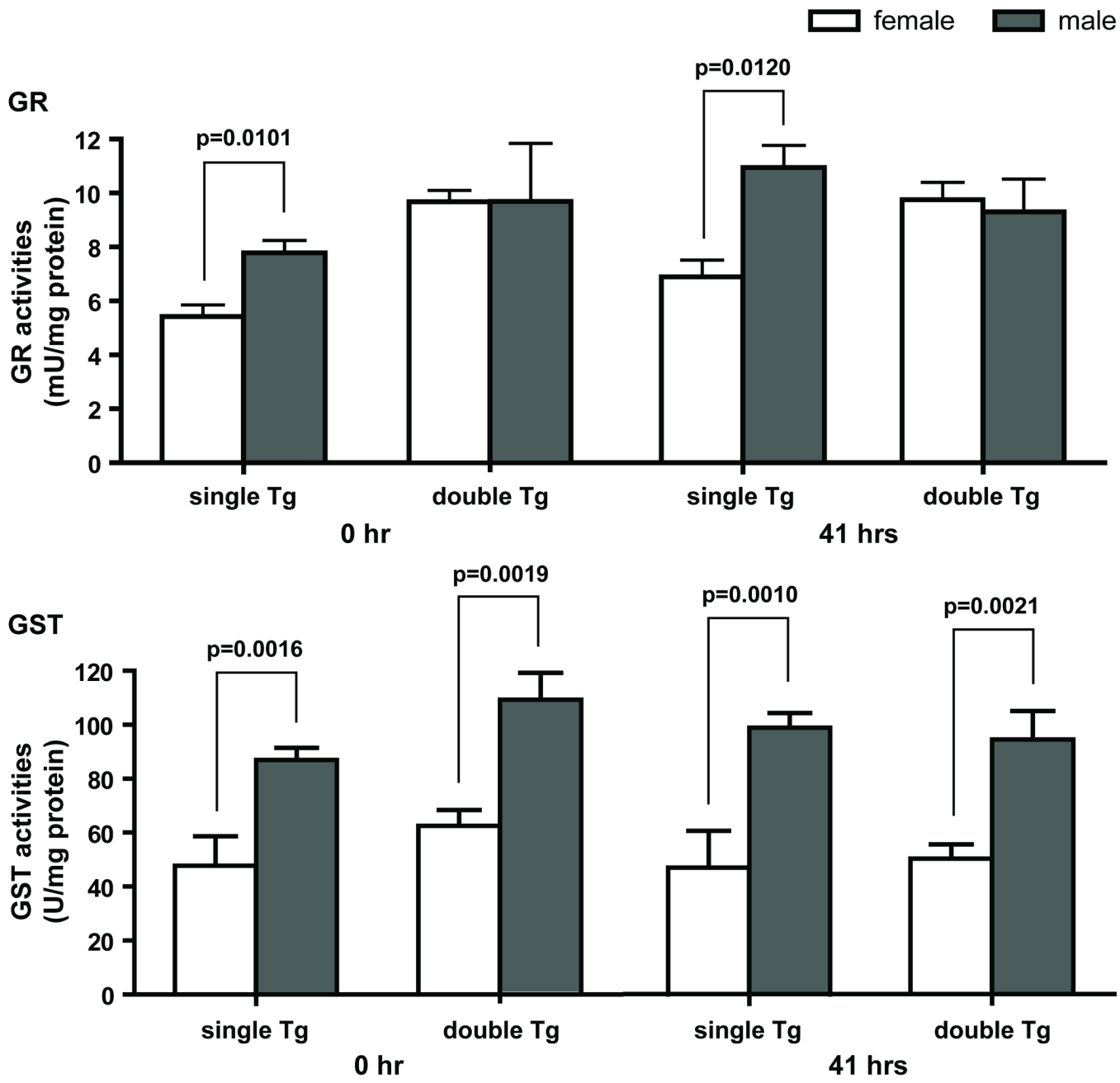

Figure 7.

Gender differences in GR and GST activities. Upper panel, significant differences in GR activities between males and females were observed in single Tg mice at both time points. GR activities in male single Tg mice were 40 and 60% higher than that in females at 0 and 41 hours, respectively. Lower panel, significant differences in GST activities between males and females were observed in single and double Tg mice at both 0 and 41 hours. On the average, GST activities in male mice were 80 to 110% higher than that in females. GR and GST are protein designations for glutathione reductase and glutathione S-transferase, respectively. Single Tg, n=14 (10 males and 4 females); double Tg, n=11 (4 males and 7 females). Mean ± SEM of

specific activities are shown. Student's t test was used for the comparison between males and females within each genotype.

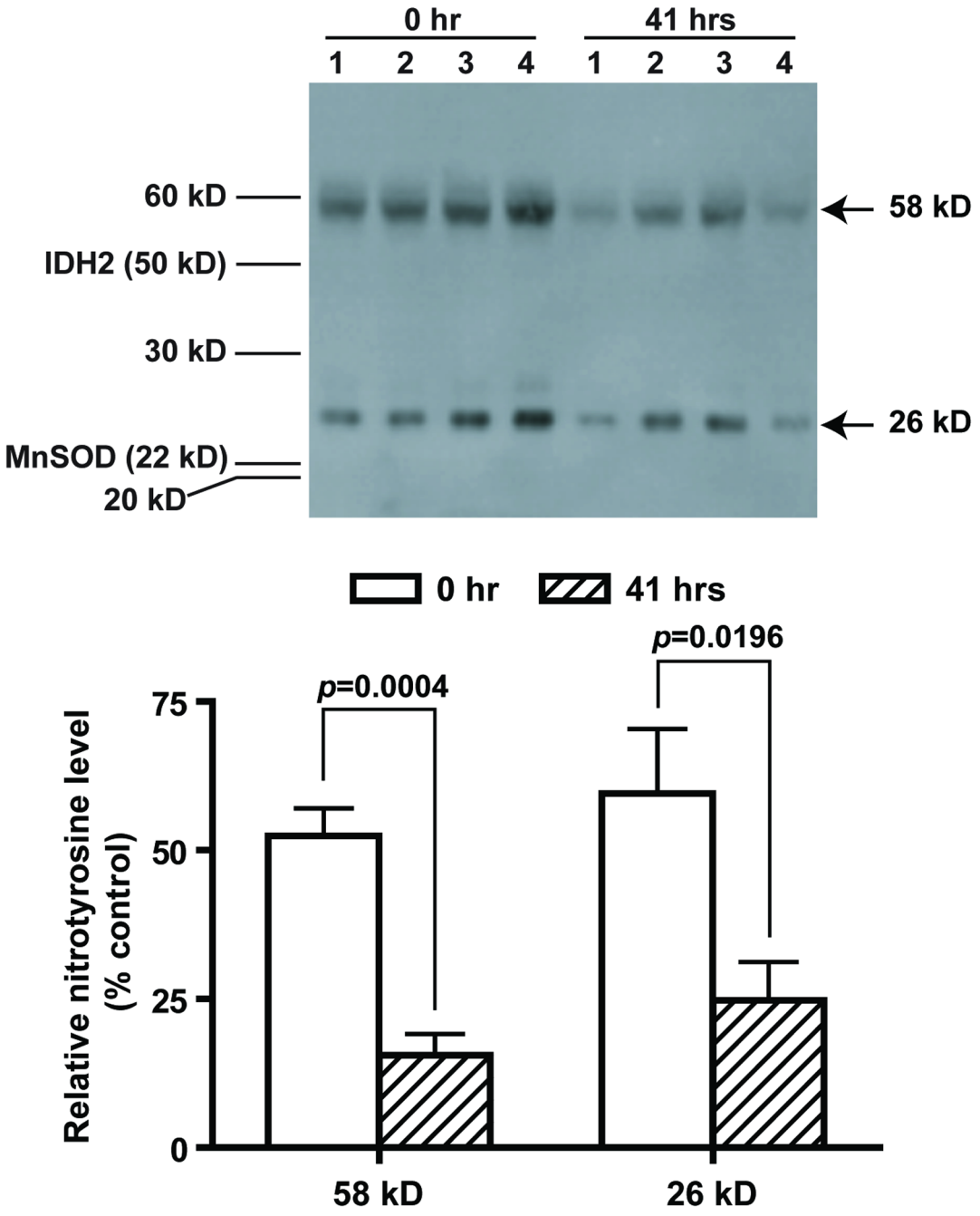

Figure 8.

Reduction of 3-nitrotyrosine in mouse livers after partial hepatectomy. Representative western blot results from four double Tg males are shown (upper panel). Signal intensities from the two major 3-nitrotyrosine positive bands were quantified and normalized to that of β-actin (lower panel). Sizes of the two major 3-nitrotyrosine positive bands were determined based on molecular weight standards and actual locations of IDH2 and MnSOD on the same blot. Paired t test was carried out for the comparison of each 3-nitrotyrosine positive band between 0- and 41-hour samples.

Table 1

Primary and secondary antibodies used in this study

Target	Origin	Company/Source	Catalog no.	Dilution
S phase cells (BrdU)	Rat monoclonal	Abcam	ab6326 BU1/75(ICR1)	2 μg/mL
Rat IgG (H+L)[1]	Rabbit polyclonal	Vector Laboratories	BA-4000	1 μg/mL
Proliferating cell nuclear antigen (PCNA)	mouse monoclonal	Dako	M0879, clone PC10	1:1,000
CuZnSOD (SOD1)	rabbit polyclonal	Lab Frontier	LF-PA0013	1:10,000
MnSOD (SOD2)	rabbit polyclonal	Stressgen	SOD-110	1:5,000
EC-SOD (SOD3)	rabbit polyclonal	custom-made[3]	ref # [80]	1 μg/mL
Peroxiredoxin 1 (PRDX1)	rabbit polyclonal	Lab Frontier	LF-PA0001	1:2,000
Peroxiredoxin 3 (PRDX3)	rabbit polyclonal	Lab Frontier	LF-PA0030	1:2,000
Thioredoxin 1 (TXN1)	rabbit polyclonal	Lab Frontier	LF-PA0002	1:2,000
Thioredoxin 2 (TXN2)	rabbit polyclonal	Lab Frontier	LF-PA0012	1:1,000
Glutathione peroxidase 1 (GPX1)	rabbit polyclonal	Lab Frontier	LF-PA0019	1:1,000
Catalase (CAT)	mouse monoclonal	Sigma	C0979, clone CAT-505	1:40,000
Cytosolic aconitase (ACO1)	rabbit polyclonal	R. Eisenstein	ref # [81]	1:2,000
Mitochondrial aconitase (ACO2)	rabbit polyclonal	R. Eisenstein	ref # [82]	1:2,000
IDH2[4]	rabbit polyclonal	custom-made[3]		0.5 μg/mL
NNT[5]	rabbit polyclonal	custom-made[3]		1 μg/mL
Nitrotyrosine	mouse monoclonal	Upstate	05–233, clone 1A6	1:2,000
β-actin[2]	mouse monoclonal	Sigma	A3854, clone AC-15	1:50,000
IRS-1	rabbit polyclonal	Cell Signaling	2382	1:1,000
Phospho-IRS-1 (Ser332/336)	rabbit polyclonal	Cell Signaling	2580	1:1,000
β-Arrestin 1	mouse monoclonal	Invitrogen/Zymed	39–5000	1:1,000
Phospho-β-Arrestin 1 (Ser412)	rabbit polyclonal	BioSource	44–200	1:1,000
Casein kinase 1ε	mouse monoclonal	Santa Cruz	Sc−81446	1:1,000
ERK1/2	rabbit polyclonal	Assay Designs	KAP-MA001	1:1,000
Phospho-ERK1/2 (Thr202/Tyr204)	rabbit polyclonal	Assay Designs	KAP-MA021	1:1,000
PI3K P110α	rabbit polyclonal	Cell Signaling	4255	1:1,000
Rb	rabbit polyclonal	Abcam	Ab6075	1:200
Phospho-Rb (Ser807)	rabbit polyclonal	Invitrogen	44–579	1:1,000
P34 Cdc2	rabbit polyclonal	Invitrogen/Zymed	33–1800	1:1,000

Target	Origin	Company/Source	Catalog no.	Dilution
Phospho-p34 Cdc2 (Thr14/Tyr15)	rabbit polyclonal	Invitrogen/Zymed	38–7300	1:1000
Mouse IgG (H+L)[2]	goat polyclonal	Bio-Rad	172–1011	1:10,000
Rabbit IgG (H+L)[2]	goat polyclonal	Bio-Rad	170–6516	1:10,000

[1] tagged with biotin

[2] tagged with HRP

[3] Proteintech Group Inc., USA

[4] Keyhole limpet hemocyanin conjugated (KLH)-N_{433}TTDFLDTIKSNLDRALGKQ$_{452}$ peptide as antigen

[5] KLH-C_{1073}DALQAKVRESYQK$_{1086}$ peptide as antigen